

Insights into source/sink controls on wood formation and photosynthesis from a stem chilling experiment in mature red maple

Tim Rademacher^{1,2,3} , Patrick Fonti⁴ , James M. LeMoine² , Marina V. Fonti^{4,5} , Francis Bowles⁶,
Yizhao Chen⁷ , Annemarie H. Eckes-Shephard^{7,8} , Andrew D. Friend⁷  and Andrew D. Richardson² 

¹Harvard Forest, Harvard University, Petersham, MA 01366, USA; ²School of Informatics, Computing and Cyber Systems and Center for Ecosystem Science and Society, Northern Arizona University, Flagstaff, AZ 86011, USA; ³Institut des Sciences de la Forêt Tempérée, Université du Québec en Outaouais, Ripon, J0V 1V0, QC, Canada; ⁴Swiss Federal Research Institute for Forest, Snow and Landscape Research WSL, Birmensdorf 8903, Switzerland; ⁵Institute of Ecology and Geography, Siberian Federal University, Krasnoyarsk 660041, Russia; ⁶Research Designs, Lyme, NH 03769, USA; ⁷Department of Geography, University of Cambridge, Cambridge, CB2 1BY, UK; ⁸Department of Physical Geography and Ecosystem Science, Lund University, Lund 223 62, Sweden

Summary

Author for correspondence:

Tim Rademacher

Email: tim.rademacher@uqo.ca

Received: 6 April 2022

Accepted: 30 July 2022

New Phytologist (2022)

doi: 10.1111/nph.18421

Key words: anatomy, growth, nonstructural carbon, phloem, sink, source, wood, xylogenesis.

- Whether sources or sinks control wood growth remains debated with a paucity of evidence from mature trees in natural settings.
- Here, we altered carbon supply rate in stems of mature red maples (*Acer rubrum*) within the growing season by restricting phloem transport using stem chilling; thereby increasing carbon supply above and decreasing carbon supply below the restrictions, respectively.
- Chilling successfully altered nonstructural carbon (NSC) concentrations in the phloem without detectable repercussions on bulk NSC in stems and roots. Ring width responded strongly to local variations in carbon supply with up to seven-fold differences along the stem of chilled trees; however, concurrent changes in the structural carbon were inconclusive at high carbon supply due to large local variability of wood growth. Above chilling-induced bottlenecks, we also observed higher leaf NSC concentrations, reduced photosynthetic capacity, and earlier leaf coloration and fall.
- Our results indicate that the cambial sink is affected by carbon supply, but within-tree feedbacks can downregulate source activity, when carbon supply exceeds demand. Such feedbacks have only been hypothesized in mature trees. Consequently, these findings constitute an important advance in understanding source–sink dynamics, suggesting that mature red maples operate close to both source- and sink-limitation in the early growing season.

Introduction

Wood – the secondary xylem and defining feature of trees – is a remarkable material. It shapes ecosystems, by enabling trees to grow tall and compete for light (Niklas, 1992); it has altered the developmental trajectory of the biosphere and earth system by serving as a slow-turnover pool of organic matter, thus sequestering atmospheric CO₂ (Pugh *et al.*, 2020); and, it has influenced the evolution of human societies and civilization by providing fuel, fiber, and building materials that are strong and light (Bros tow *et al.*, 2010). However, wood is in some ways a conundrum: while dendrochronologists, schoolchildren, and foresters all know that trees grow more in some years and less in others (Fritts, 2012), our mechanistic understanding of the underlying processes controlling inter-annual variation in wood growth is surprisingly poor, especially with regard to mature trees growing in natural settings (Rathgeber *et al.*, 2016; Friend *et al.*, 2019).

There are two ways in which environmental factors might influence wood growth (xylogenesis) and these are reflected in the two dominant paradigms: either wood growth is controlled by carbon supply – from current photosynthesis, which may be supplemented from reserves – i.e. ‘source-limited,’ or wood growth is controlled by the activity of the lateral meristem, through the direct impact of limiting (environmental or internal) factors on the processes of xylogenesis, i.e. ‘sink-limited’ (Körner, 2003). The source-limited hypothesis is the basis of most vegetation models (Fatichi *et al.*, 2014; Körner, 2015; Friend *et al.*, 2019), but there is more and more evidence for direct environmental limitations on the cambium (Körner, 2006; Parent *et al.*, 2010; Peters *et al.*, 2020). A consequence of the sink-limited hypothesis is the existence of feedback mechanisms from sinks to sources that will cause source activity (photosynthesis) to be downregulated when sink activity (xylogenesis) is inadequate to meet supply (Walker *et al.*, 2021).

While distinguishing between source- and sink-limitation might seem straightforward, in practice it is not (Gessler & Grossiord, 2019). This is because at either extreme, xylogenesis must be either source- or sink-limited. Clearly carbon supply must be a

top-down constraint on growth, as wood growth can never exceed carbon supply. However, at the same time there must be an upper limit on growth (G_{\max} ; Fig. 1a), controlled by the maximum sink activity and independent of carbon supply. What is

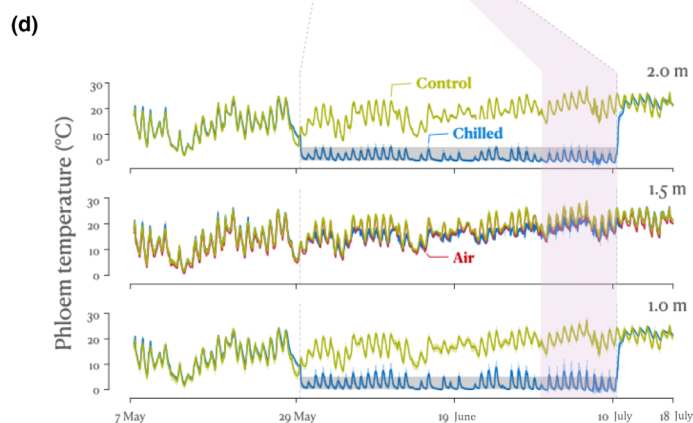
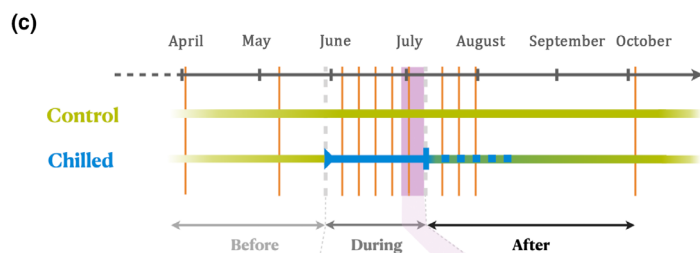
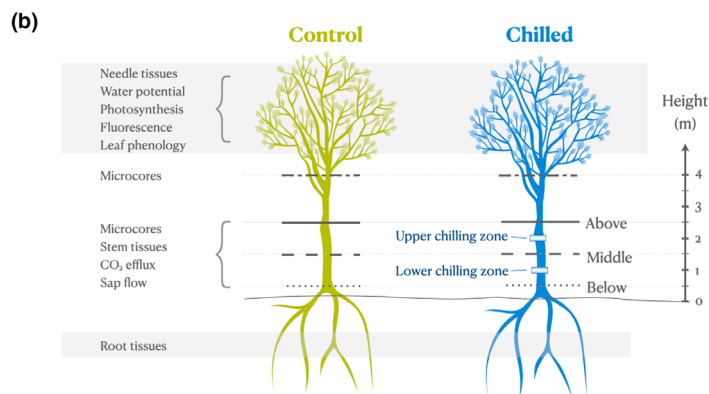
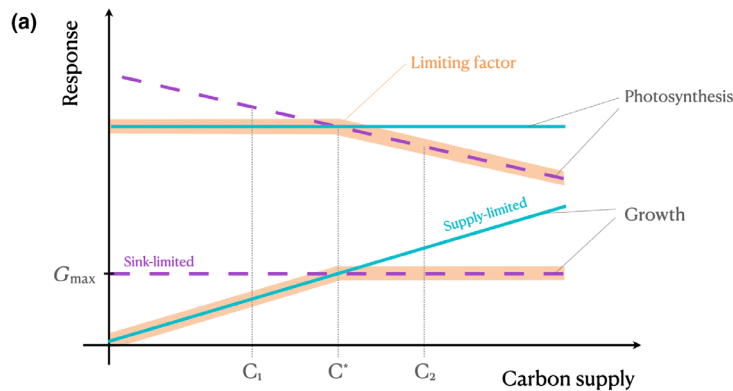


Fig. 1 (a) Conceptual responses of radial wood growth and photosynthesis to changes in carbon supply under supply-limitation (turquoise lines; C_1) vs sink-limitation (purple lines; C_2) with orange shading indicating the overall limitation, which may switch over time. C^* indicates point where growth and photosynthesis switch between being supply- vs sink-limited. G_{\max} indicates a theoretical maximum growth rate. (b) Experimental setup including tissue sampling locations, (c) timeline of treatments including start and end dates of chilling (gray vertical dashed lines), wood growth and nonstructural carbon sampling dates (orange vertical lines), and the period of photosynthesis measurements (purple rectangle), and (d) mean temperatures for the air (red line), the phloem of chilled trees (blue line), and the phloem of control trees (green line).

needed are experimental designs that offer the opportunity to identify whether under ambient environmental conditions source- or sink-limitation is dominant in various species, ecosystems, and phenophases. Conceptually, a tree could operate under either limitation and possibly switch between them over time (Fig. 1a). In this framework, a transition from supply-limited growth to sink-limited growth occurs at a supply level of C^* (Fig. 1a). With our present knowledge of carbon dynamics and xylogenesis, however, it is not known whether trees are more generally operating below C^* (where growth is supply-limited, e.g. C_1), above C^* (where growth is sink-limited, e.g. C_2), or close to C^* ; possibly even switching between supply- and sink-limitation over time due to internal and/or external factors (e.g. developmental or environmental constraints). Trees may have evolved to operate under long-term homeostasis in their environmental niche (i.e. supply in equilibrium with demand) with feedbacks maintaining this homeostasis.

Previous studies have provided mixed results in support of these competing views. Girdling experiments, which show reductions in growth below the girdle (reduced supply) and increases in growth above the girdle (enhanced supply), suggest that wood growth is supply-limited (Wilson, 1968; Maier *et al.*, 2010). But, at the whole-tree level, CO_2 enrichment, which would be expected to enhance carbon supply to the entire tree because of stimulated photosynthesis, has not generally been shown to result in increased wood growth in mature trees (Jiang *et al.*, 2020; Lauriks *et al.*, 2021), supporting the sink-limitation hypothesis (and pointing to within-tree feedbacks downregulating photosynthetic activity). Other experimental studies have equally shown that wood growth is reduced following exposure to low atmospheric CO_2 (Huang *et al.*, 2021), experimentally induced defoliation (Deslauriers *et al.*, 2015; Wiley *et al.*, 2017), as well as natural defoliation resulting from pest outbreaks (Castagneri *et al.*, 2020). However, these growth responses could simply result from severe supply-limitation (e.g. C_1): they tell us nothing about whether sink-limitation occurs more generally.

Here, we used an experimental manipulation – applying the ‘phloem chilling’ method of Johnsen *et al.* (2007) and De Schepper *et al.* (2011) – to regulate the carbon flow to different points along the stem of mature red maples (*Acer rubrum*). As phloem flow is modulated by temperature (Jensen *et al.*, 2016), phloem transport can be temporarily and reversibly blocked by chilling the phloem close to $0^\circ C$ (Gould *et al.*, 2004; Peuke *et al.*, 2006; Thorpe *et al.*, 2010). An advantage of this approach is that unlike traditional girdling approaches, phloem chilling does not cause wounding and is reversible (Rademacher *et al.*, 2019). We installed chilling collars at 1.0 and 2.0 m to create a gradient of carbon supply along the stem and isolate one stem section (between 1 and 2 m) from both recent assimilates from the canopy and root reserves (Fig. 1b). Our focus here is on this alteration of carbon supply below, between, and above the transport restrictions, rather than on the growth response under each collar (e.g. 1 and 2 m), where near-freezing temperatures constitute an acute limitation (Fig. 1d). We used microcores to observe the seasonal progression of xylogenesis, and we also characterized stem respiration and concentrations of stored nonstructural carbon (NSC)

to quantify local carbon dynamics. Leaf-level measurements of photosynthesis, and visual observations of leaf phenology (i.e. bud burst, leaf elongation, leaf coloration, and leaf fall) were used to assess the impact of any within-tree feedback mechanisms. Ultimately, whether a tree is source- or sink-limited may vary over time, especially when differences in source and sink phenologies may cause temporary carbon surpluses or deficits in shoulder seasons. Here, we focused on the early growing season (29 May–10 July 2019), when trees appear to be particularly sensitive to phloem transport manipulations (Maier *et al.*, 2010; De Schepper *et al.*, 2011).

Based on the concepts presented earlier (Fig. 1a), we hypothesized that if wood growth is supply-limited (C_1), then in our treatments we should see reductions of growth at 1.5 m (the isolated stem section) and possibly at 0.5 m (depending on root reserve depletion) but enhancements of growth at 2.5 m (conclusion: reject sink-limited hypothesis, under current environmental conditions). If, however, wood growth is sink-limited (C_2), then our treatments should have no effect on growth at any height (conclusion: reject supply-limited hypothesis, under current environmental conditions). A third possibility is that under current environmental conditions, trees are operating in the vicinity of C^* . In this case, we might see reduced growth at 1.5 m in response to reduced carbon supply, but no response at 2.5 m in response to enhanced carbon supply (conclusion: joint limitation of growth by supply-limitation and sink-limitation). Finally, feedbacks could downregulate source activity (evidenced through potential changes in photosynthetic activity and/or leaf phenology) as a result of the build-up of phloem carbon above the top chilling collar (conclusion: within-tree feedbacks can modulate photosynthesis to control supply in response to demand). We expect that all treatment effects will gradually accumulate during the chilling treatment, but will taper off after the chilling is ended (i.e. after the peak growing season to avoid the complete halt of wood growth; Fig. 1c). Understanding the role of source–sink dynamics of large trees in natural settings under ambient environmental conditions is important because of their importance as a sink in the global carbon cycle (Pugh *et al.*, 2019) and the fact that source–sink interactions in large trees are different from small trees (Hartmann *et al.*, 2018). Our experiment provides a rare look into the source–sink interactions of mature trees in a natural temperate forest.

Materials and Methods

Study site and species

Red maple (*A. rubrum*) is widespread throughout eastern North America, and of great cultural and commercial importance. At Harvard Forest in central Massachusetts, USA, red maple is together with red oak the most dominant species in a mixed forest. We studied a cohort of eight mature trees growing in close proximity (within 20 m of each other) in the Prospect Hill Tract ($42^\circ 30.8'N$, $72^\circ 13.1'W$, 350 m above sea level) on sandy acidic loam. These 75 ± 1.7 (mean \pm SD) year-old trees regenerated naturally after a stand-replacing hurricane in 1938. They have experienced an average temperature of $8.0 \pm 0.7^\circ C$ and annual

precipitation of 1096 ± 228 mm over the past 57 yr (Boose & Gould, 2019) reaching an average diameter of breast height of 24.2 ± 1.2 cm and a mean height of 22.6 ± 1.0 m. The experiment was performed in 2019, a relatively wet year with 270 mm above the average of the instrumental record and directly followed the wettest year on record with 1840 mm. Annual mean temperature in 2019 was close to the long-term average with 7.9°C . Overall, neither the preceding year, nor the year of the experiment, showed strong climatic constraints.

Chilling setup

We separated the cluster of eight trees into four pairs, with each two trees of similar size and canopy status (Supporting Information Notes S1). We randomized which tree of each pair was subjected to phloem chilling at 1.0 and 2.0 m (Fig. 1b). To monitor phloem temperatures, negative temperature coefficient thermistors (2.5 mm diameter, SC30F103V; Amphenol Thermometrics Inc., St Marys, PA, USA) were placed into the phloem, one each at 1.0 and 2.0 m using surgical needles in early May 2019. Around the same time, we also installed heat-pulse sap flow sensors (East 30, Pullman, WA, USA) at 1.5 m, which measure sap flow at three depths (i.e. 5.0, 17.5, and 30.0 mm). In mid-May, we wrapped 3/8" type L copper tubing 30 times around stems to produce 30-cm-wide chilling collars (centered on the chilling height), which were linked to a coolant supply line using one ALPHA2 circulator (Grundfos, Bjerringbro, Denmark) for each tree (i.e. supplying two chilling collars). To chill the trees, coolant – a mix of water and polypropylene glycol – was constantly circulated through the main supply line and the chilling collars from a reservoir that was cooled to maintain a temperature of roughly 0°C with a six-ton chiller using a 1.5 horse power circulation pump (Chillking, Bastrop, TX, USA). During the chilling period, 20 thermistors (T₁₀₉; Campbell Scientific, Logan, UT, USA), which were calibrated in an ice-bath before deployment, were used to monitor air temperature, temperatures of the supply lines, and at the chilling collars. Piping and chilling collars were insulated (e.g. bubble wrap, glass wool, piping insulation) and covered in radiative barriers. The chilling was switched on at midday on 29 May 2019 and switched off at midday on 10 July 2019, reducing phloem temperatures to an average of $2.8 \pm 2.6^\circ\text{C}$ at 1.0 m and 1.4 ± 1.8 at 2.0 m in chilled trees over this 42-d period. Phloem temperatures in chilled trees at 1.0 and 2.0 m were 15.4 and 16.8°C lower than the control group during this chilling period, but only 2.3°C lower at 1.5 m, suggesting that the chilling effects were mainly local but there was some diffusion (i.e. mostly up stem with xylem sap flow during the day). At 1.5 m phloem temperature of control trees closely followed air temperature ($R^2 = 0.98$). During the chilling, phloem temperatures at 1.0 and 2.0 m were maintained in the range 0 – 5°C for 84% and 97% of the time.

Physiological monitoring

We monitored wood formation and resulting anatomy, NSC concentrations in leaves, stems and roots, stem CO_2 efflux, sap

flow, leaf phenology, as well as leaf and branch water potential throughout the 2019 growing season (Fig. 1b). Wood formation was assessed from thin-section (7 μm -thick cross-sectional cuts), which were obtained from microcores collected at 0.5, 1.5, 2.5, and 4.0 m throughout the 2019 growing season (see Fig. 2a for sampling dates) and one follow-up sample on 4 August 2020. Microcores were stored in a solution of 75% ethanol and 25% glacial acetic acid for 24 h after collection. Then, they were transferred to 95% ethanol until they were embedded in paraffin (Tissue Processor 102; Leica Biosystems, Wetzlar, Germany), stained with astra-blue and safranin, and cut with a rotary microtome (RM2245; Leica Biosystems). Images of the thin-sections were scanned at a resolution of *c.* $1.5 \text{ pixels } \mu\text{m}^{-1}$ (Axioscan Z1; Zeiss, Jena, Germany) and ring widths were measured using the Wood Image Analysis and Database (Rademacher *et al.*, 2021c; Seyednasrollah *et al.*, 2021). To compare differences in growth between sampling locations, we fitted monotonic general additive models to each growth series using the SCAM v.1.2-9 package (Pya, 2020). For each growth series, we identified the start of wood formation as the date halfway between the sampling dates of the last microcore without and the first microcore with signs of cell enlargement. To estimate the cell-wall area in one end-of-season image, we converted a region of interest for the 2018 and 2019 ring to grayscale and used a threshold to differentiate between lumen areas and cell-wall areas. Regions of interest were maximized for each ring, while excluding rips and tears in the sample image. We reported results for a brightness threshold of 0.8, but varying thresholds between 0.7 and 0.9 did not change the patterns. Cell-wall area estimates, based on the brightness threshold procedure, were converted to mass using a cell-wall density of 1.459 g cm^{-3} for red maple (Kellogg & Wangaard, 1969). Vessels were identified in each region of interest after denoising the image using the determinant of Hessian operator (Lindeberg, 2015) as implemented in the *imbhessian* function of the IMAGER package (Barthelme & Ochi, 2020). We added a minimum size threshold of $500 \mu\text{m}^2$ to differentiate between large fiber lumina and small vessel lumina. An illustration of the methods can be found in Notes S2.

For NSC analysis, we collected tissue samples from roots; stems at 0.5, 1.5, and 2.5 m; and sun-exposed leaves throughout the growing season. We froze them on dry ice and transferred them to a freezer (-60°C) as soon as possible before they were eventually freeze-dried (FreeZone 2.5; Labconco, Kansas City, MO, USA with a Hybrid Vacuum Pump; Vaccubrand, Wertheim, Germany), ground (mesh 20; Thomas Scientific Wiley Mill, Swedesboro, NJ, USA), and homogenized (Spex SamplePrep 1600; MiniG, Metuchen, NJ, USA). Root and stem samples were collected using an increment corer (5.15 mm; Hagöf, Långele, Sweden), while several sun-exposed leaves were cut with pruning shears from a bucket lift. For roots, we sampled one large coarse root per tree repeatedly at least 1 m below the root collar and 15 cm from any previous sampling location. All the xylem tissue was homogenized for each root sample. For stem samples, we separated phloem tissue (including sieve elements and phloem parenchyma), the outer bark, and the first

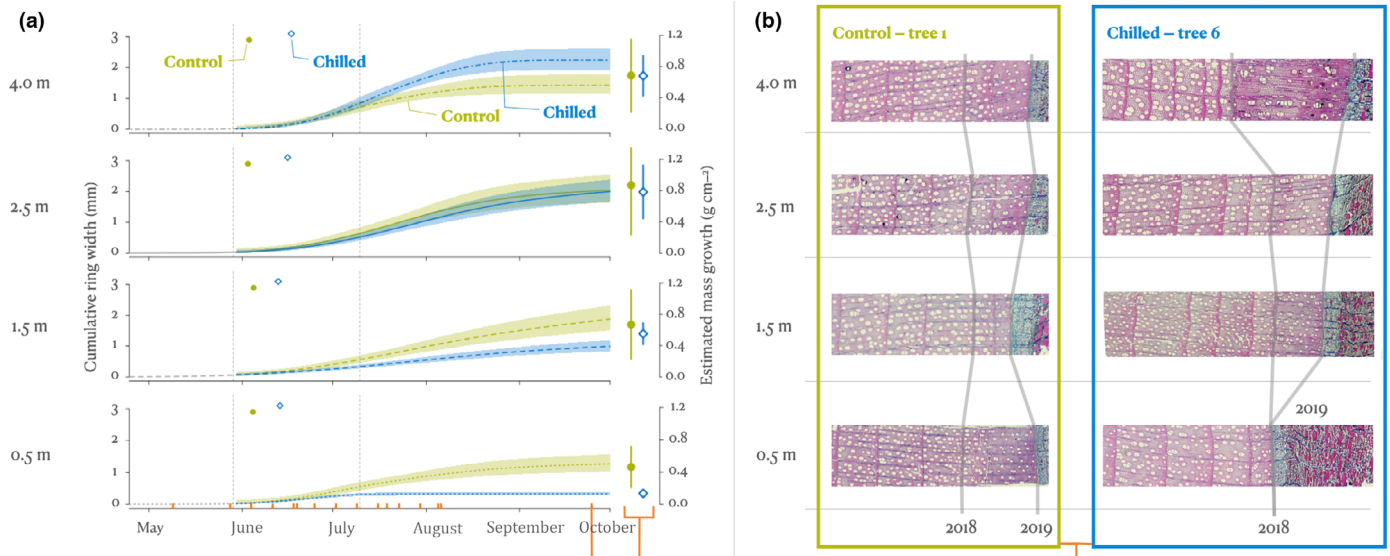


Fig. 2 (a) Dynamics of radial growth in chilled (blue) vs control trees (green) at 4.0, 2.5, 1.5, and 0.5 m. Lines and shading illustrate the mean and one standard error of a general additive model fitted to the four trees in each treatment. The mean start of the growing season (i.e. visual observation from microcores) is indicated at the top of each panel as small blue diamonds for chilled trees and small green dots for control trees. The mean estimated annual radial mass increment per 1 cm² cross-sectional area (close to area of a typical increment core) and one standard error are displayed on the right as large blue diamonds and bars for chilled trees and large green dots and bars for control trees. Gray dashed vertical lines show the start and end of the chilling period and orange tick marks on the x-axis denote sampling dates. (b) Images of thin-sections from 25 September for one control (tree 1 on left) and chilled tree (tree 6 on right). The images were rescaled to keep growth of the previous years relatively constant. The two gray lines indicate the final ring boundaries of the 2018 and 2019 rings, demarcating the growing season that included our chilling experiment. Unscaled, uncropped, and high-resolution versions of the images can be found in the Supporting Information Notes S2.

centimeter of the xylem and homogenized them separately. We used an established protocol for colorimetric analysis of soluble sugar and starch concentrations using phenol–sulfuric acid after ethanol extraction (Landhäusser *et al.*, 2018). Absorbances were read twice for each sample at 490 nm for sugar and 525 nm for starch using a spectrophotometer (Genesys 10S UV-Vis; Thermo Fisher Scientific, Waltham, MA, USA). To calibrate absorbance measurements with 1 : 1 : 1 glucose : fructose : galactose curves for sugars and glucose curves for starch (Sigma, St Louis, MO, USA) we used the R package NSCPROCESSR (<https://github.com/TTRademacher/NSCprocessR>). For overall quality control, we used laboratory control standards of red oak stem wood (Harvard Forest, Petersham, MA, USA) and potato starch (Sigma Chemicals). Batches of 40 samples always included at least seven blanks and nine laboratory control standards. The control standards had coefficients of variation of 0.08 and 0.12 for red oak soluble sugar and starch concentrations and 0.07 for potato starch.

To quantify the relationship between chilling and basic tree metabolism, we also measured stem CO₂ efflux. Every week throughout the growing season, we measured CO₂ efflux at 0.5, 1.5, and 2.5 m on all trees generally from 13:00 to 14:00 h GMT-4. We measured chambers in the same order to facilitate comparison over longer timescales by minimizing differences in diurnal fluctuations. Carbon dioxide (CO₂) concentrations were measured with a closed-chamber attached to an Infra-red gas analyser (Li-820; Li-Cor, Lincoln, NE, USA) at 1 Hz once the chamber internal CO₂ concentration had stabilized at ambient

levels (Carbone *et al.*, 2019) and converted to fluxes with uncertainties using the RESPCHAMBERPRO package (Perez-Priego *et al.*, 2015).

We monitored leaf phenology of all eight red maples, plus six additional red maples in the stand in 2018 and 2019 according to the protocol by O’Keefe (2019). Using binoculars, we visually observed the crown of each tree to determine the dates of bud burst, leaf elongation, leaf coloration, and leaf fall. During the period with green leaves, we also measured pre-dawn leaf and branch water potential approximately every second week to estimate potential effects of the chilling on tree water status (in addition to the sap flow sensors; Notes S3).

During the last 10 d of the chilling, we conducted a campaign to compare photosynthesis and chlorophyll fluorescence in chilled and control trees (purple highlight in Fig. 1c,d). Instantaneous photosynthetic rates ($n = 46$), light response curves, and A/C_i curves were measured in shade or sun leaves of each pair of trees (i.e. one control and one chilled tree) simultaneously using two Li-Cor-6400 from a bucket lift. We estimated photosynthetic parameters (maximal rate of photosynthetic electron transport or J_{max} and maximal rate of RuBisCO carboxylation activity or V_{cmax}), by fitting A/C_i curves to the data using the PLANTECO-PHYS package (Duursma, 2015). Directly after each photosynthesis measurement, we also removed the leaf and measured chlorophyll fluorescence (OS-30P; Opti-Sciences, Hudson, NH, USA). Then, we wrapped each leaf in aluminum foil and kept it in a cooler with ice to dark-adapt. In the evening of each day, we re-measured chlorophyll fluorescence in dark-adapted leaves,

to estimate stress to the photosynthetic apparatus (Maxwell & Johnson, 2000).

Statistical analysis

All statistical analyses were performed in R v.3.6.3 (R Core Team, 2019). The data and code to reproduce all results are publicly available on the Harvard Forest Data Archive (Rademacher *et al.*, 2021b). We used mixed effects models that were fitted using the LME4 package (Bates *et al.*, 2015) with tree identifiers as a random variable, and a fixed treatment effect. For data with various data points along the stem, we include a sampling height and treatment interaction as a proxy carbon supply gradient. When measurement series over time were compared, we also include datetime as a categorical fixed effect and its interaction with the treatment or the treatment and sampling height interactive effect in the case of stem data. We refrain from reporting significance based on arbitrary *P*-values in line with the philosophy of the LME4 package, as the degrees of freedom of mixed effects models are nontrivial and can only be estimated (Bates *et al.*, 2015). Instead, we report estimated mean effects and their standard errors ($\hat{\mu} \pm \hat{\sigma}_{\hat{\mu}}$) or relative differences between these (in percent) unless specified otherwise.

Results

Changes to carbon supply and NSC concentrations

We altered phloem transport by chilling stem sections as shown by changes in local phloem sugar concentrations. Phloem sugar concentrations were similar between treatment groups before chilling, but increased above the chilling collars (Fig. 3a). Phloem sugar concentration increased during the chilling by 13% ($0.35 \pm 0.35\%$ dry weight), 18% ($0.50 \pm 0.35\%$ dry weight), and 34% ($0.92 \pm 0.36\%$ dry weight) at 0.5, 1.5, and 2.5 m, respectively. In contrast, phloem starch concentrations increased above the chilling collars by an average 37% during the chilling treatment ($0.25 \pm 0.20\%$ dry weight) and decreased by 64% below the two chilling collars ($0.43 \pm 0.18\%$ dry weight). It is likely that some starch was remobilized to supplement phloem sugar depleted as a result of the flow restrictions. While NSC concentrations in the phloem, particularly soluble sugar, showed treatment effects (Fig. 3a), bulk NSC concentrations in stems and roots across the first centimeter of xylem tissue varied comparatively little between the control and chilled trees before, during and after the chilling (Fig. 4).

Changes to wood growth

The chilling-induced restriction of phloem transport affected radial wood growth along the stem, with wider rings forming in regions of increased carbon supply and narrower rings forming in regions of reduced carbon supply (Fig. 2a,b). Over the five preceding years and the year following the experiment, both control and chilled trees showed little pre-existing variation in growth with sampling height (standard deviation of 0.1 and

0.2 mm for control and chilled groups). Control trees continued to grow without systematic variation with sampling height at an average ring width of 1.9 ± 0.6 mm in 2019 (Fig. 2b). Chilled trees grew 84% less below the two phloem restrictions (0.3 ± 0.1 mm), 26% less below one phloem restriction (1.4 ± 0.3 mm), and 16–21% more above the restrictions (2.2 ± 1.0 mm at 2.5 m and 2.3 ± 0.9 mm at 4 m). Despite the more than seven-fold difference in ring width between 4.0 and 0.5 m in chilled trees (difference in mean estimated effect from mixed effects model), intra-annual growth dynamics (i.e. general shape of the growth curve) were largely similar between control and chilled trees with no abrupt reduction during the chilling (Fig. 2a). However, we did observe a 12 ± 4 -d delay in the onset of wood formation in chilled trees relative to control trees (see dots in Fig. 2a).

The estimated effect of the carbon supply gradient on mass growth was less clear than the effect on ring width, but some changes in the underlying wood anatomy emerged (Table 1): below the chilling collars vessel density and percentage of cell-wall area were higher, whereas only vessel density was clearly lower than controls above the chilling. Like ring width, mass growth, based on a single end-of-season microcore, was substantially less at 0.5 m in chilled trees than controls. In contrast to ring width, mass growth showed no significant increases between chilled and control trees at 1.5, 2.5 or 4.0 m (Fig. 2a). Wood anatomy showed substantial variation among trees and sampling dates (Table 1; Notes S2). Strangely, both the vessel density (i.e. number of vessels per mm^2 cross-sectional) and the percentage of cell-wall area had a tendency to decline with carbon supply, whereas vessel lumen area was relatively constant across samples (Table 1). Vessels have a lower cell-wall to lumen area ratio than fibers. Thus, fewer vessels of similar size per cross-sectional area at higher carbon supply in chilled trees might be expected to result in a higher overall percentage of cell-wall area. However, the estimated percentage of cell-wall area at higher carbon supply covaried positively with vessel density (Table 1). Although small, the net changes in the percentage of cell-wall area and large variability in wood anatomy attenuated treatment-induced differences in ring width at high carbon supply (Fig. 2a).

Changes to stem CO₂ efflux

Stem CO₂ efflux responded rapidly to the chilling treatment (Fig. 5). Within a week after the start of chilling, stem CO₂ efflux per unit stem surface area started diverging between chilled and control trees at all stem heights (Fig. 5). Reductions in CO₂ efflux in chilled compared to control trees averaged 52% below two restrictions ($-0.43 \pm 0.22 \mu\text{mol m}^{-2} \text{s}^{-1}$), 26% below one restriction ($-0.22 \pm 0.22 \mu\text{mol m}^{-2} \text{s}^{-1}$), and 38% above both restrictions ($-0.31 \pm 0.22 \mu\text{mol m}^{-2} \text{s}^{-1}$) over the chilling period. Once the chilling was switched off, stem CO₂ efflux of chilled trees converged with the control group within 1 or 2 wk below both one and two restrictions (Fig. 5). However, above the upper restriction stem CO₂ efflux of the chilled group increased strongly averaging about twice those of the control group for the

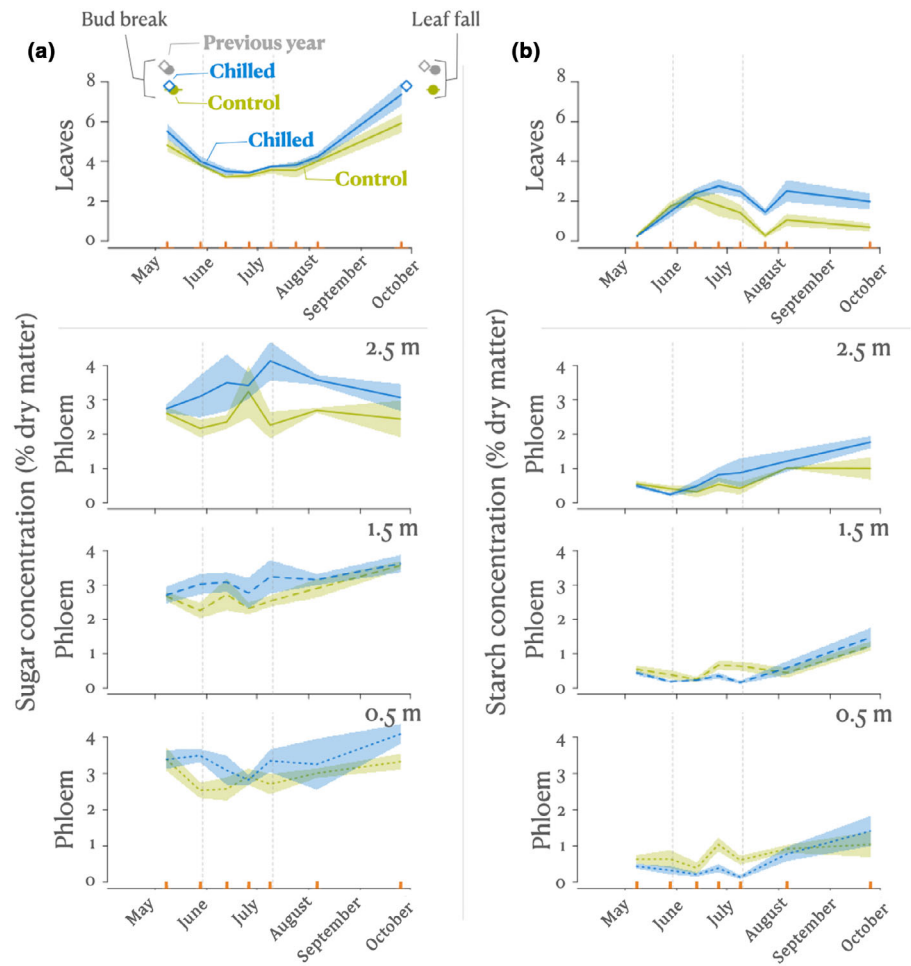


Fig. 3 (a) Mean soluble sugar and (b) starch concentrations for chilled (blue) and control trees (green) as measured in the leaves and phloem tissues at 2.5, 1.5, and 0.5 m. Shading displays one standard error of the mean. The switching on and off of the chilling is indicated by gray vertical dashed lines and orange tick marks on the bottom x-axis denote sampling dates. In the leaf soluble sugar graph (top left panel), blue diamonds and green dots and their associated error bars represent the mean and one standard deviation of the dates of bud break and leaf fall for the chilled and control trees in year of the experiment, respectively. Gray symbols indicated the phenological dates for each group in the year preceding the experiment.

next 3 months, before converging towards the end of the growing season (Fig. 5).

Leaf-level changes

In addition to multiple effects at the stem-level, we found an accumulation of leaf NSC, a downregulation of photosynthetic capacity, and earlier leaf coloration and fall in chilled trees (Figs 3, 6). During the chilling, leaf NSC concentrations started to diverge between treatments, culminating in increases in leaf sugar and starch concentrations of +14% ($0.65 \pm 0.25\%$ dry weight) and +168% ($1.31 \pm 0.31\%$ dry weight) relative to the controls (Fig. 3). While we only measured photosynthesis shortly after the summer solstice (i.e. last week of chilling, 29 June–10 July; Fig. 1c) when leaf starch concentrations just started to diverge between treatments (Fig. 3), maximal rates of photosynthetic electron transport (J_{\max}) and RuBisCO carboxylase activity (V_{\max}) as estimated from A/C_i curves declined with chilling (Fig. 6): V_{\max} was $46.6 \pm 1.5 \mu\text{mol m}^{-2} \text{s}^{-1}$ for chilled trees compared with $52.1 \pm 1.7 \mu\text{mol m}^{-2} \text{s}^{-1}$ for control trees, J_{\max} was $85 \mu\text{mol m}^{-2} \text{s}^{-1}$ for chilled compared to $97 \mu\text{mol m}^{-2} \text{s}^{-1}$ for control trees, and dark respiration was 5% higher in chilled trees relative to control (Fig. 6). Despite these differences in photosynthetic parameters, we did not detect any changes in

instantaneous photosynthetic rates or light response curves between the two treatments (Notes S4). Likewise, we did not detect a significant treatment effect on ratios of variable fluorescence over maximum fluorescence in dark-adapted leaves (Notes S4). In addition to changes in leaf NSC and photosynthetic capacity, we also observed significantly earlier leaf coloration by 12 ± 2 d and leaf fall by 16 ± 2 d for chilled trees compared to control trees (Fig. 3). There were no effects of chilling on the tree water status as per leaf and branch water potentials and sap flow measurements (Notes S3).

Discussion

Phloem carbon supply determines early-season wood growth

The pronounced local differences in final ring width along the carbon supply gradient suggest a direct supply-limitation in the early-growing season (C_1 in Fig. 1a). The effect is unlikely to be a direct cold-inhibition of growth, as the cooling was localized (e.g. only 2.3°C difference to ambient at 1.5 m) and a direct cold-inhibition would have affected all sampling heights equally, being equidistant to the cooling collars. Natural and artificial defoliation experiments support the idea that reduced carbon

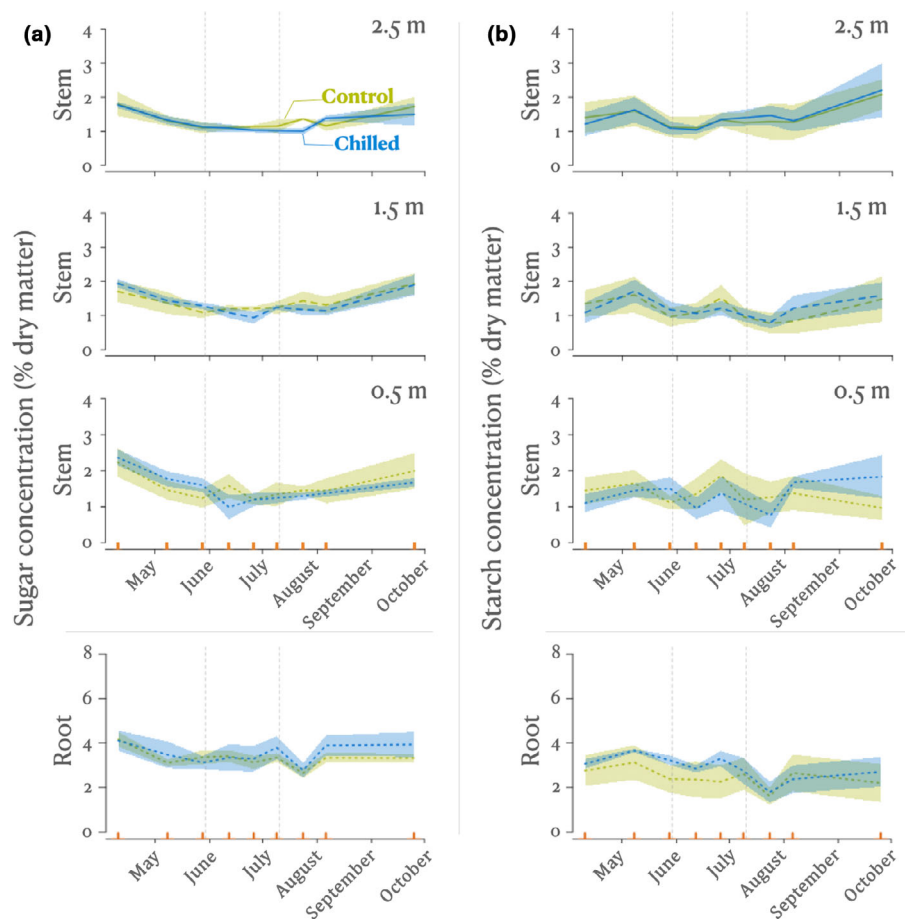


Fig. 4 (a) Mean soluble sugar and (b) starch concentrations for chilled (blue lines) and control trees (green lines) as measured in the outermost centimeter of the xylem at 2.5, 1.5, and 0.5 m, and roots. Shading displays one standard error of the group mean. The switching on and off of the chilling is indicated by gray vertical dashed lines and orange tick marks on the bottom x-axis denote sampling dates.

supply can limit wood formation (Deslauriers *et al.*, 2015; Wiley *et al.*, 2017; Castagneri *et al.*, 2020). Previous phloem transport experiments have shown that ring width is affected by both low and high carbon supply (Wilson, 1968; Goren *et al.*, 2004; Maier *et al.*, 2010). We have also shown that both ring width and biomass of white pine respond to mid- to late-season girdling and phloem compression (Rademacher *et al.*, 2021a). The fact that we saw a much clearer effect on ring width may be due to the early season timing of the treatment, when effects on cell division and elongation are likely more pronounced than on cell-wall thickening, and hence mass increment. Effects on volume growth have also been shown to be particularly strong under early-season drought stress (D'Orangeville *et al.*, 2018; Martínez-Sancho *et al.*, 2022) and phloem transport manipulations (Maier *et al.*, 2010; De Schepper *et al.*, 2011). A treatment effect on carbon sequestration (i.e. mass growth) instead of ring width (i.e. volume growth) was only detectable in the present study under severe carbon supply-limitation below two chilling collars, with no clear effect at increased carbon supply. This could suggest that trees operate close to C^* , which seems a likely evolutionary outcome given a co-limited process (McMurtrie & Dewar, 2013; Franklin *et al.*, 2020); however, maintenance of such as joint limitation would require regulating feedbacks. Overall, we conclude that volume growth (and possibly mass growth) in red maple exhibit carbon supply-limitations in the early growing season.

Although ring width was associated with the spatial carbon supply gradient, there was no abrupt halt or reduction in growth as a result of the chilling. In fact, the shape of the intra-annual growth curve was similar for both treatments (Fig. 2a). Intra-annual wood development in conifers is known to be strongly constrained by endogenous factors, which results in typical gradual transitions of cell characteristics in seasonally-limited habitats (Buttò *et al.*, 2020, 2021). The smooth shape of the observed intra-annual growth curve, despite the abrupt chilling and hence phloem transport restriction, supports an important role of endogenous factors on wood formation in this diffuse-porous angiosperm. Studies investigating xylogenesis and resulting anatomy in angiosperms are still rare (Balzano *et al.*, 2018; Arnič *et al.*, 2021) and comparing angiosperms and conifers is not simple, because of important physiological differences, such as a higher proportion of parenchyma cells in angiosperms (Spicer, 2014). While anatomical characteristics were not the primary focus of this work, we found little evidence for carbon supply-related changes in vessels density and the characteristics of fibers. Mean supply of carbon to the cambium has been shown to mainly affect cell division rate for white pine (Rademacher *et al.*, 2021a), and the most parsimonious explanation for our results are systematic changes in cell proliferation rate (i.e. both fibers and vessels), thus cell numbers, with carbon supply rate. We did not detect an effect of carbon supply on the ratio of vessel to

Table 1 Estimated treatment effects using a mixed effects model fitted using the restricted maximum likelihood procedure in the LME4 package (Bates *et al.*, 2015) in R (R Core Team, 2019).

Effect	Ring width (mm)	ρ_{vessel} ($n \text{ mm}^{-2}$)	r_{vessel} (μm)	Percentage cell-wall area (%)	m (g cm^{-2})
Intercept	858 ± 804 (1.1)	80 ± 13 (6.1)	22.7 ± 1.8 (12.4)	43.9 ± 3.3 (13.5)	0.43 ± 0.03 (13.9)
2019	1049 ± 734 (1.4)	-28 ± 14 (-2.0)	-1.4 ± 1.3 (1.1)	-9.5 ± 3.6 (-2.6)	-0.09 ± 0.04 (-2.5)
2019 : X : 4.0 m	419 ± 1137 (0.4)	-16 ± 18 (-0.9)	-0.5 ± 2.6 (-0.2)	-2.9 ± 4.6 (-0.6)	-0.03 ± 0.04 (-0.6)
2019 : C : 2.5 m	696 ± 734 (0.9)	14 ± 14 (1.0)	-0.6 ± 1.3 (-0.5)	0.9 ± 3.6 (0.2)	0.01 ± 0.04 (0.2)
2019 : X : 2.5 m	284 ± 1137 (0.3)	-11 ± 18 (-0.6)	0.2 ± 2.6 (0.1)	2.1 ± 4.6 (0.5)	0.02 ± 0.04 (0.5)
2019 : C : 1.5 m	-183 ± 734 (-0.3)	-10 ± 13 (-0.7)	1.2 ± 1.4 (0.8)	1.5 ± 3.6 (0.4)	0.01 ± 0.04 (0.4)
2019 : X : 1.5 m	-494 ± 1137 (-0.4)	-2 ± 18 (-0.1)	2.7 ± 2.6 (1.1)	7.5 ± 4.6 (1.6)	0.07 ± 0.04 (1.7)
2019 : C : 0.5 m	371 ± 734 (-0.5)	-16 ± 15 (-1.1)	0.2 ± 1.3 (0.1)	-4.1 ± 4.0 (-1.0)	-0.05 ± 0.04 (-1.3)
2019 : X : 0.5 m	-1567 ± 1137 (-1.4)	3 ± 18 (0.2)	1.1 ± 2.6 (0.4)	5.0 ± 4.6 (1.1)	0.05 ± 0.04 (1.1)
2018 : X : 4.0 m	-42 ± 1137 (-0.0)	1 ± 18 (0.0)	0.2 ± 2.6 (0.1)	1.2 ± 4.6 (0.3)	0.01 ± 0.04 (0.3)
2018 : C : 2.5 m	-74 ± 734 (-0.1)	-29 ± 14 (-2.1)	-0.3 ± 1.3 (-0.3)	-9.6 ± 3.6 (-2.6)	-0.09 ± 0.04 (-2.6)
2018 : X : 2.5 m	-29 ± 1137 (-0.0)	-16 ± 18 (-0.9)	2.4 ± 2.6 (0.9)	1.5 ± 4.6 (0.3)	0.01 ± 0.04 (0.3)
2018 : C : 1.5 m	-95 ± 734 (-0.1)	-20 ± 14 (-1.5)	1.0 ± 1.4 (0.7)	-3.1 ± 3.6 (-0.8)	-0.03 ± 0.04 (-0.8)
2018 : X : 1.5 m	-26 ± 1137 (-0.0)	-15 ± 18 (-0.8)	2.7 ± 2.6 (1.0)	2.2 ± 4.6 (0.5)	0.02 ± 0.04 (0.5)
2018 : C : 0.5 m	166 ± 734 (0.2)	25 ± 15 (-1.7)	2.5 ± 1.3 (2.0)	-2.2 ± 4.0 (-0.5)	0.00 ± 0.04 (0.1)
2018 : X : 0.5 m	653 ± 1137 (0.6)	-23 ± 18 (-1.2)	1.4 ± 2.6 (0.5)	-0.8 ± 4.6 (-0.2)	-0.01 ± 0.04 (-0.2)

Each model contained tree identifier as a random effect plus the listed intercepts and fixed effects for which we provide the mean effect, its standard error, and the t -value in the following format: $\hat{\mu} \pm \sigma_{\hat{\mu}}$ (t -value). 'X' stands for chilled treatment (light blue cell background) and 'C' for control treatment. '2019' and '2018' stand for categorical variable of year and sampling height are listed as 0.5 m (below restrictions), 1.5 m (in-between restrictions), 2.5 and 4.0 m (above restrictions). We tested effects on ring width, vessel density (ρ_{vessel}), estimated vessel radius (r_{vessel}), estimated percentage cell-wall area, and estimated mass contained in ring (m) on the microcore images collected on 25 September 2019.

fibers, but these results are inconclusive due to the large between-sample variability. Differences in the sensitivities of vessel and fiber formation to carbon supply in angiosperms may have important consequences for water transport and carbon sequestration, thus presenting an important avenue of further research. Because systematic changes in wood anatomy with carbon supply would change the relationships between ring width (e.g. the most prevalent measure of wood growth) and mass, they could prove important in understanding how much carbon will be sequestered by nonconiferous trees in the future.

Carbon supply and temperature have both also been found to influence the critical dates and dynamics of wood formation (Oribe *et al.*, 2001; Rossi *et al.*, 2008; Rohde *et al.*, 2011; Balducci *et al.*, 2016; Cuny & Rathgeber, 2016). While the effect of temperature on the onset of wood formation is generally assumed to be cumulative over the dormancy period (Huang *et al.*, 2020), we observed a delay in the onset of wood growth in chilled trees although bud break had occurred roughly at the same time as the controls, possibly suggesting immediate and direct effect of temperature on cambial activation. Alternatively, local changes in phloem NSC concentrations could be responsible for the different timings, as NSC reserves have been linked to resumption of growth for several angiosperms (Amico Roxas *et al.*, 2021). Reserves were also important in *Larix*, where in a cambial heating experiment, cambial activity resumed but then stopped when local starch reserves were used up (Oribe & Funada, 2017). However, here carbon supply only changed gradually once the transport bottleneck was induced and phloem sugar concentrations had not diverged yet between chilled and control trees. Moreover, the delay was similar across sampling heights, but the carbon supply and temperature gradients were not. Consequently, some additional signal is required to explain consistent

delay along the stem or this may simply be a pre-existing difference between-group difference. Targeted manipulative experiments to better understand the role of temperature and carbon status on wood phenology at various points throughout the growing season, especially in angiosperms, are clearly still needed.

Sink feedbacks downregulate source activity

Our findings at the stem-level provide strong evidence for a direct control of carbon supply on lateral meristem activity for red maple in the early growing season, yet we also found multiple lines of evidence for source-sink feedbacks. Looking at source tissues in leaves, we found an accumulation of NSC, a downregulation of photosynthetic capacity, and a shortened leaf season for the chilled trees, all suggesting a coupling between the supply-controlled lateral meristem and source tissues. We saw cumulative increases in leaf sugar and starch concentrations of the chilled trees compared to the control group, culminating in large differences towards the end of the season (Fig. 3). Although trees appear to be able to load the phloem against strong concentrations gradients (Gersony *et al.*, 2021), the gradual NSC accumulation in leaves over the season presumably resulted from the backup of carbon transport in the phloem in chilled red maple, which is best characterized as a passive phloem loader (Eschrich & Fromm, 1994) like about half of all characterized tree species (Liesche, 2017). Higher NSC concentrations in turn have been theorized to inhibit photosynthesis (Salmon *et al.*, 2020), which has long been confirmed in herbaceous plants and tree leaves (Iglesias *et al.*, 2002; Vaughn *et al.*, 2002), but lacked evidence along the long transport pathways between the trunk at breast height and the canopy of mature trees. We only measured photosynthesis during the last week of chilling, when leaf sugar and

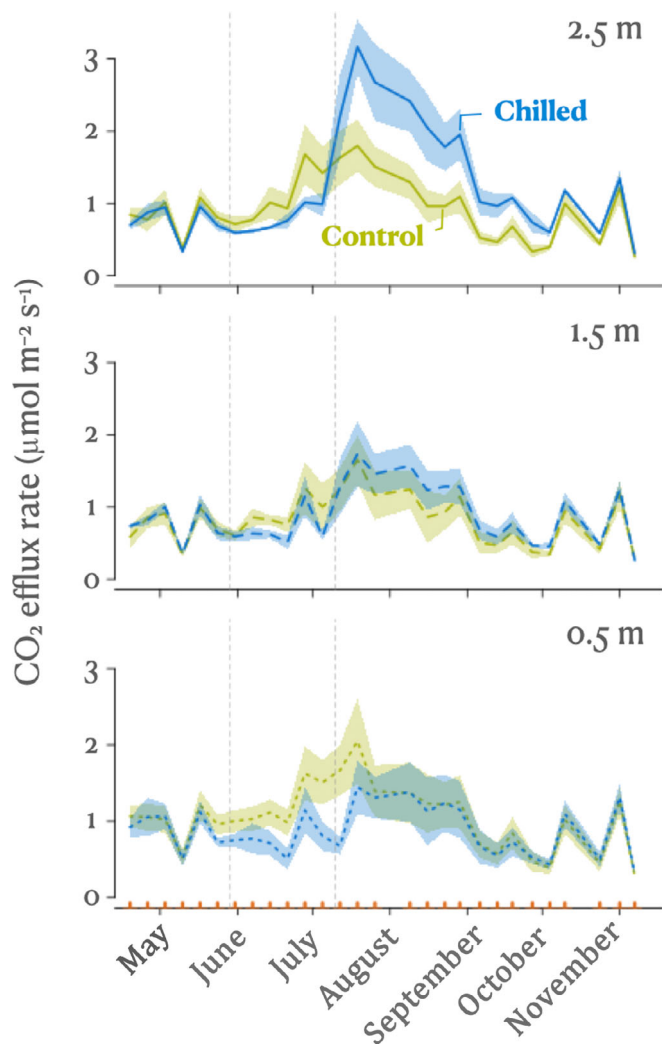


Fig. 5 Weekly mean stem CO₂ efflux rates on a stem-area basis for chilled (blue lines) and control trees (green lines) as measured throughout the season. Shading displays one standard error of the mean. The switching on and off of the chilling is indicated by gray vertical dashed lines and orange tick marks on the x-axis denote sampling dates.

starch concentrations just started to diverge between the chilled and control trees. Arguably, leaf NSC concentrations had not increased sufficiently to result in a detectable change in instantaneous photosynthetic rates or light response curves. Nonetheless, we already observed declines in the photosynthetic capacity (i.e. J_{\max} and V_{cmax}).

Beyond the changes in photosynthetic capacity, increased leaf NSC concentrations may have caused the significant observed advancement of leaf coloration and fall for chilled trees compared to controls. This advancement stands in contrast to very similar dates of leaf coloration and fall in the previous year. This effect on leaf phenology is very unlikely to have arisen from a direct temperature-limitation, because chilling ended almost 3 months before leaf coloration and was limited to small parts of the stem. Accumulation of NSC towards the end of the season has previously been linked to advancement of leaf coloration and fall in the closely related sugar maple (Murakami *et al.*, 2008), yet free-

air CO₂ enrichment experiments consistently observe increases in photosynthesis, hence carbon supply, without clear advancement of leaf coloration or fall (Norby, 2021). The apparent discrepancy may be reconciled if the accumulation of leaf NSC causes the observed effects on leaf phenology directly, as such an accumulation has generally not been observed in free-air CO₂ enrichment experiments (Norby, 2021). Here, radial growth above both restrictions may have attained an upper limit (e.g. G_{\max} in Fig. 1a), which led to the tree shifting from being source-limited (C_1) to sink-limited (C_2). This would suggest that the trees were operating close to C^* (Fig. 1a). NSC may have accumulated in the phloem and leaves, as a consequence of this growth limitation. Independent of what caused the increase in leaf NSC, the observed advancement of leaf phenology constitutes a third indication of source–sink coupling, whereby leaf-on period, hence source activity, is constrained due to a carbon-mediated feedback from sinks. Although the differences in photosynthetic capacity between the two groups did not lead to marked differences in instantaneous assimilation rates in the last week of chilling, they may have increased later in the growing season (concurrently with the observed gradual leaf NSC accumulation) and could sum to a substantial difference in carbon fixation over the entire growing season. Any effect on carbon assimilation would be compounded by the advanced leaf coloration and fall. Together the increases in leaf NSC, the early downregulation of photosynthetic capacity, and the advancement of autumn leaf phenology provide strong evidence for a feedback inhibition in mature forest trees.

Local carbon dynamics show temporal decoupling of treatment effects

Leaf NSC concentrations changed gradually over the entire growing season, whereas stem CO₂ efflux responded much quicker to the chilling treatment. These varying response scales highlight the need for continuous monitoring to be able to disentangle the complexity of the observed experimental effects. Carbon supply can either be sourced directly from recent assimilates or from NSC reserves, that can build up and be remobilized over multiple years (Carbone *et al.*, 2013; Muhr *et al.*, 2016). Like in other phloem transport manipulations (Maier *et al.*, 2010; Regier *et al.*, 2010; Rademacher *et al.*, 2021a), bulk NSC concentrations in stems and roots (here measured in the first centimeter of the stem and roots) reacted more sluggishly and show little to no treatment effect (Fig. 4). However, below both restrictions NSC remobilization and/or reduced sink activity compensated for the reduced phloem carbon transport to maintain phloem sugar concentrations. This supports the idea that at low carbon supply, sugar concentrations near the cambium are homeostatically maintained within relatively tight limits that vary seasonally (Huang *et al.*, 2021; Rademacher *et al.*, 2021a). Such homeostasis is typical in biological systems and likely evolved to ensure metabolic stability for inter-annual wood formation given the role of soluble sugar concentrations as a signal, resource and possible driver of wood formation (Riou-Khamlichi *et al.*, 2000; Lastdrager *et al.*, 2014; Carteni *et al.*, 2018). Across the developing xylem, NSC concentrations vary markedly (Uggla *et al.*,

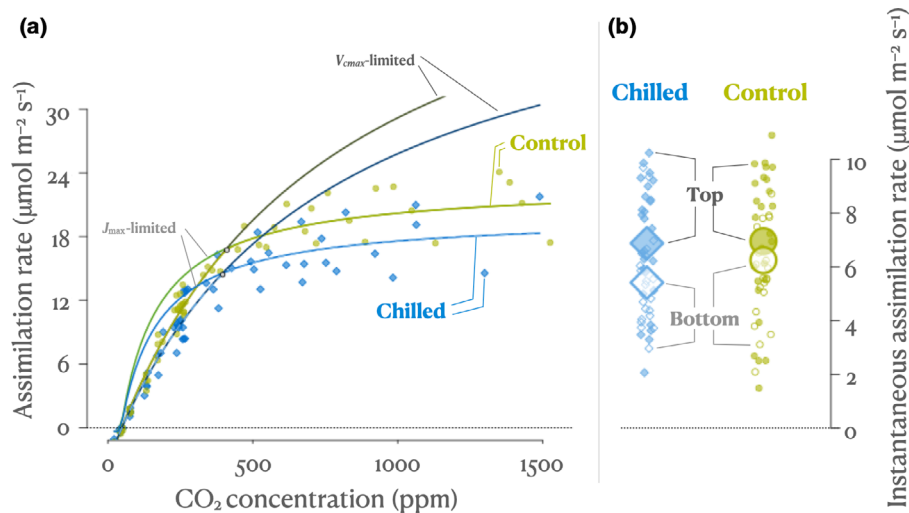


Fig. 6 (a) A/C_i curves of chilled (blue) and control trees (green) as measured during the last week of the chilling period. Line brightness corresponds to the limiting factor with dark lines showing maximal rate of RuBisCO carboxylation activity (V_{cmax})-limited curves, intermediate colors showing maximal rate of photosynthetic electron transport (J_{max})-limited curves and bright lines showing the combined limitation. Control trees have slightly higher J_{max} and V_{cmax} values compared with chilled trees. (b) Paired measurements ($n = 46$) of instantaneous assimilation rates showed slightly higher rates for control trees (green dots) at the bottom of the canopy (open symbols) relative to chilled trees (blue diamonds), while sun-leaves (filled symbol) did not show any differences. Large symbols give the respective group mean for instantaneous rates (i.e. top chilled, bottom chilled, top control, and bottom control) in (b).

2001). Given that we observed contrasting reactions of NSCs in adjacent tissues, such as phloem and stem soluble sugar, it begs the question whether these gradients remain stable under varying conditions or whether only particular aspects of the gradient, such as phloem concentrations, are maintained. Repeated and spatially highly resolved measurements of NSC concentrations, using techniques such as Raman spectroscopy (Gersony *et al.*, 2021), promise to advance our understanding of these gradients and their dynamics in response to internal and external factors. These gradients are likely to be crucial to understanding the impact of carbon dynamics on specific processes of wood formation (e.g. cambial activity, cell enlargement, and cell-wall thickening). In contrast to reduced carbon supply, we did not observe a substantial accumulation of bulk NSCs in stems at elevated carbon supply throughout the growing season. While this can be interpreted as further evidence that the cambium is carbon supply-limited (e.g. any additional carbon is used for growth; C_1), some coordination is needed to avoid the depletion of reserves that are crucial for winter survival (Vitasse *et al.*, 2014), spring emergence (Amico Roxas *et al.*, 2021), and defense against various stressors (Wiley *et al.*, 2017). Nonetheless, our findings support the idea that NSC reserves are not simply an overflow store of energy (Martínez-Vilalta *et al.*, 2016) that can be rapidly accessed when required, as they remain very stable even when carbon supply is acutely restricted.

The observed changes in stem CO_2 efflux correspond to imposed temperatures during the chilling period and then the carbon supply gradient thereafter, suggesting that local metabolic activity is more sensitive to changes in temperature than to changes in carbon supply. Nonetheless, the spike in CO_2 efflux post-chilling supports the idea that the first pulse of phloem-transported carbon after the restriction is lifted is metabolized locally (possibly to fuel wall-thickening). Measurements of CO_2

efflux may include some portion that is transported in the xylem from adjacent regions (Teskey *et al.*, 2008). However, given that xylem transported CO_2 has been shown to decrease in trees with severed phloem transport (Bloemen *et al.*, 2014), and CO_2 solubility decreases with temperature (Servio & Englezos, 2001), we suspect that the observed changes in CO_2 efflux mainly represent local metabolic activity. Respiration is long known to respond to both temperature and substrate concentrations (Amthor, 2000). The observed pattern is likely a combination of reduced respiration during the chilling and a spike in metabolic activity as a response to stopping the chilling. Interestingly, the large and immediate changes in CO_2 efflux suggest that local metabolic activity and growth can be somewhat decoupled temporarily or spatially, as CO_2 efflux was lower when radial volume growth was higher at high carbon supply (e.g. 2.5 m) in chilled trees relative to control during the chilling period. Our results appear to indicate that trees seem to operate close to C^* (Fig. 1a), understanding the regulating interactions between sources and sinks is a key component of understanding the mechanisms of wood formation.

Conclusions

We found evidence for a carbon supply-limitation of the activity of the lateral meristem as well as multiple source–sink feedbacks in mature red maple trees. These feedbacks can reconcile the apparent discrepancy arising from previous phloem transport manipulations (Wilson, 1968; De Schepper *et al.*, 2011; Rademacher *et al.*, 2021a) and defoliation experiments (Deslauriers *et al.*, 2015; Castagneri *et al.*, 2020) that showed carbon supply-limitation of the lateral meristem, with whole-tree level CO_2 enrichment that suggested a sink-limitation at increased carbon supply (Körner *et al.*, 2005). Our results illustrate how within-

tree feedbacks can reduce carbon assimilation when phloem sugar concentrations increase as a result of phloem transport manipulations in mature red maples. These findings suggest that trees operate close to both source- and sink-limitation and may switch between them. While our results are based on a single species at one location, they identify potential mechanisms for reconciling apparently contrasting evidence with regard to the control of wood growth. More work is needed to evaluate whether these findings can be extrapolated to other species, sites, ecosystems, environmental conditions, or phenophases. Our work highlights the need to integrate evidence from multiple tissues (i.e. leaves and phloem, xylem in stems and roots) across entire growing seasons when investigating source–sink interactions. Otherwise, conclusions about source–sink interactions (e.g. from single tissues or over short periods) can be mistaken because local and whole-tree effects can be temporarily decoupled. Importantly, our identification of strong source–sink interactions even in unstressed conditions refute the prevailing source-centric paradigm as used in most current models representing mature trees in natural settings.

Acknowledgements

TR, ADR, ADF and YC acknowledge support from the Natural Environment Research Council – National Science Foundation International Collaboration program under grant nos. NE/P011462/1 and DEB-1741585. ADR and TR also acknowledge the support from the National Science Foundation under grants DEB-1237491 and DEB-1832210. The authors thank David Basler, Teemu Hölltä, Henrik Hartmann and Christian Körner for discussion of the ideas, Mark von Scoy, Elise Miller, and Shawna Greyeyes for help in the field, and Shawna Greyeyes, Amberlee Pavey and Angelina Valenzuela for help in the laboratory. The authors also thank David Basler for sharing the orthomosaics of the site. AHE-S acknowledges support from the European Research Council under the European Union Horizon 2020 programme (758873). This study contributes to the strategic research areas BECC and MERGE.

Author contributions

TR and ADR designed the experiment with input from JML, ADF, YC, PF and AHE-S. TR and FB built the chilling apparatus. TR conducted and supervised the fieldwork. TR, MVF, JML and PF processed the samples. TR analyzed the data, produced the figures and wrote a first draft. All co-authors discussed ideas, provided feedback, edited the manuscript draft and approved the manuscript for submission.

ORCID

Yizhao Chen  <https://orcid.org/0000-0002-9218-6679>
Annemarie H. Eckes-Shephard  <https://orcid.org/0000-0002-2453-3843>
Marina V. Fonti  <https://orcid.org/0000-0002-2415-8019>
Patrick Fonti  <https://orcid.org/0000-0002-7070-3292>

Andrew D. Friend  <https://orcid.org/0000-0002-9029-1045>
James M. LeMoine  <https://orcid.org/0000-0002-1702-8339>
Tim Rademacher  <https://orcid.org/0000-0002-0627-6564>
Andrew D. Richardson  <https://orcid.org/0000-0002-0148-6714>

Data availability

The data and code to reproduce all results are publicly available on the Harvard Forest Data Archive as data set hf421 (<https://harvardforest1.fas.harvard.edu/exist/apps/datasets/showData.html?id=HF421>).

References

- Amico Roxas A, Orozco J, Guzmán-Delgado P, Zwieniecki MA. 2021. Spring phenology is affected by fall non-structural carbohydrate concentration and winter sugar redistribution in three Mediterranean nut tree species. *Tree Physiology* 41: 1425–1438.
- Amthor JS. 2000. The McCree–de Wit–Penning de Vries–Thornley respiration paradigms: 30 years later. *Annals of Botany* 86: 1–20.
- Arnič D, Gričar J, Jevšenak J, Božič G, von Arx G, Prislán P. 2021. Different wood anatomical and growth responses in European beech (*Fagus sylvatica* L.) at three forest sites in Slovenia. *Frontiers in Plant Science* 12: 669229.
- Balducci L, Cuny HE, Rathgeber CBK, Deslauriers A, Giovannelli A, Rossi S. 2016. Compensatory mechanisms mitigate the effect of warming and drought on wood formation: wood formation under warming and drought. *Plant, Cell & Environment* 39: 1338–1352.
- Balzano A, Cufar K, Battipaglia G, Merela M, Prislán P, Aronne G, De Micco V. 2018. Xylogenesis reveals the genesis and ecological signal of IADFs in *Pinus pinea* L. and *Arbutus unedo* L. *Annals of Botany* 121: 1231–1242.
- Barthelme S, Ochi S. 2020. IMAGER: image processing library based on 'Clmg'. [WWW document] URL <http://dahtah.github.io/imager/> [accessed 1 August 2022].
- Bates D, Mächler M, Bolker B, Walker S. 2015. Fitting linear mixed-effects models using lme4. *Journal of Statistical Software* 67: 1–48.
- Bloemen J, Agneessens L, Van Meulebroek L, Aubrey DP, McGuire MA, Teskey RO, Stepe K. 2014. Stem girdling affects the quantity of CO₂ transported in xylem as well as CO₂ efflux from soil. *New Phytologist* 201: 897–907.
- Boose E, Gould E. 2019. *Harvard Forest climate data since 1964*. Harvard Forest Data Archive. [WWW document] URL <https://harvardforest1.fas.harvard.edu/exist/apps/datasets/showData.html?id=hf300> [accessed 1 August 2022].
- Brostow W, Datashvili T, Miller H. 2010. Wood and wood derived materials. *Journal of Materials Education* 32: 125–138.
- Buttò V, Deslauriers A, Rossi S, Rozenberg P, Shishov V, Morin H. 2020. The role of plant hormones in tree-ring formation. *Trees* 34: 315–335.
- Buttò V, Rozenberg P, Deslauriers A, Rossi S, Morin H. 2021. Environmental and developmental factors driving xylem anatomy and micro-density in black spruce. *New Phytologist* 230: 957–971.
- Carbone MS, Czimczik CI, Keenan TF, Murakami PF, Pederson N, Schaberg PG, Xu X, Richardson AD. 2013. Age, allocation and availability of nonstructural carbon in mature red maple trees. *New Phytologist* 200: 1145–1155.
- Carbone MS, Seyednasrollah B, Rademacher T, Basler D, Le Moine JM, Beals S, Beasley J, Greene A, Kelroy J, Richardson AD. 2019. FLUX PUPPY – an open-source software application and portable system design for low-cost manual measurements of CO₂ and H₂O fluxes. *Agricultural and Forest Meteorology* 274: 1–6.
- Carteni F, Deslauriers A, Rossi S, Morin H, De Micco V, Mazzoleni S, Giannino F. 2018. The physiological mechanisms behind the earlywood-to-latewood transition: a process-based modeling approach. *Frontiers in Plant Science* 9: 1053.

- Castagneri D, Prendin AL, Peters RL, Carrer M, von Arx G, Fonti P. 2020. Long-term impacts of defoliator outbreaks on larch xylem structure and tree-ring biomass. *Frontiers in Plant Science* 11: 1078.
- Cuny HE, Rathgeber CBK. 2016. Xylogenesis: coniferous trees of temperate forests are listening to the climate tale during the growing season but only remember the last words! *Plant Physiology* 171: 306–317.
- De Schepper V, Vanhaecke L, Steppe K. 2011. Localized stem chilling alters carbon processes in the adjacent stem and in source leaves. *Tree Physiology* 31: 1194–1203.
- Deslauriers A, Caron L, Rossi S. 2015. Carbon allocation during defoliation: testing a defense-growth trade-off in balsam fir. *Frontiers in Plant Science* 6: 338.
- D'Orangeville L, Maxwell J, Kneeshaw D, Pederson N, Duchesne L, Logan T, Houle D, Arseneault D, Beier CM, Bishop DA *et al.* 2018. Drought timing and local climate determine the sensitivity of eastern temperate forests to drought. *Global Change Biology* 24: 2339–2351.
- Duursma RA. 2015. PLANTECOPHYS – an R package for analysing and modelling leaf gas exchange data. *PLoS ONE* 10: e0143346.
- Eschrich W, Fromm J. 1994. Evidence for two pathways of phloem loading. *Physiologia Plantarum* 90: 699–707.
- Fatichi S, Leuzinger S, Körner C. 2014. Moving beyond photosynthesis: from carbon source to sink-driven vegetation modeling. *New Phytologist* 201: 1086–1095.
- Franklin O, Harrison SP, Dewar R, Farrior CE, Brännström Å, Dieckmann U, Pietsch S, Falster D, Cramer W, Loreau M *et al.* 2020. Organizing principles for vegetation dynamics. *Nature Plants* 6: 444–453.
- Friend AD, Eckes-Shephard AH, Fonti P, Rademacher T, Rathgeber CBK, Richardson AD, Turton RH. 2019. On the need to consider wood formation processes in global vegetation models and a suggested approach. *Annals of Forest Science* 76: 49.
- Fritts H. 2012. *Tree rings and climate*. New York, NY, USA: Academic Press.
- Gersony JT, McClelland A, Holbrook NM. 2021. Raman spectroscopy reveals high phloem sugar content in leaves of canopy red oak trees. *New Phytologist* 232: 418–424.
- Gessler A, Grossiord C. 2019. Coordinating supply and demand: plant carbon allocation strategy ensuring survival in the long run. *New Phytologist* 222: 5–7.
- Goren R, Huberman M, Goldschmidt EE. 2004. Girdling: physiological and horticultural aspects. *Horticultural Reviews* 30: 1–36.
- Gould N, Minchin PEH, Thorpe MR. 2004. Direct measurements of sieve element hydrostatic pressure reveal strong regulation after pathway blockage. *Functional Plant Biology* 31: 987–993.
- Hartmann H, Adams HD, Hammond WM, Hoch G, Landhäusser SM, Wiley E, Zaehle S. 2018. Identifying differences in carbohydrate dynamics of seedlings and mature trees to improve carbon allocation in models for trees and forests. *Environmental and Experimental Botany* 152: 7–18.
- Huang J, Hammerbacher A, Gershenson J, van Dam NM, Sala A, McDowell NG, Chowdhury S, Gleixner G, Trumbore S, Hartmann H. 2021. Storage of carbon reserves in spruce trees is prioritized over growth in the face of carbon limitation. *Proceedings of the National Academy of Sciences, USA* 118: e2023297118.
- Huang J-G, Ma Q, Rossi S, Biondi F, Deslauriers A, Fonti P, Liang E, Mäkinen H, Oberhuber W, Rathgeber CBK *et al.* 2020. Photoperiod and temperature as dominant environmental drivers triggering secondary growth resumption in Northern Hemisphere conifers. *Proceedings of the National Academy of Sciences, USA* 117: 20645–20652.
- Iglesias DJ, Lliso I, Tadeo FR, Talon M. 2002. Regulation of photosynthesis through source: sink imbalance in citrus is mediated by carbohydrate content in leaves. *Physiologia Plantarum* 116: 563–572.
- Jensen KH, Berg-Sørensen K, Bruus H, Holbrook NM, Liesche J, Schulz A, Zwieniecki MA, Bohr T. 2016. Sap flow and sugar transport in plants. *Reviews of Modern Physics* 88: 035007(63).
- Jiang M, Medlyn BE, Drake JE, Duursma RA, Anderson IC, Barton CVM, Boer MM, Carrillo Y, Castañeda-Gómez L, Collins L *et al.* 2020. The fate of carbon in a mature forest under carbon dioxide enrichment. *Nature* 580: 227–231.
- Johnsen K, Maier C, Sanchez F, Anderson P, Butnor J, Waring R, Linder S. 2007. Physiological girdling of pine trees via phloem chilling: proof of concept. *Plant, Cell & Environment* 30: 128–134.
- Kellogg RM, Wangaard FF. 1969. Variation in the cell-wall density of wood. *Wood and Fiber Science* 1: 180–204.
- Körner C. 2003. Carbon limitation in trees. *Journal of Ecology* 91: 4–17.
- Körner C. 2006. Plant CO₂ responses: an issue of definition, time and resource supply. *New Phytologist* 172: 393–411.
- Körner C. 2015. Paradigm shift in plant growth control. *Current Opinion in Plant Biology* 25: 107–114.
- Körner C, Asshoff R, Bignucolo O, Hättenschwiler S, Keel SG, Peláez-Riedl S, Pepin S, Siegwolf RTW, Zott G. 2005. Carbon flux and growth in mature deciduous forest trees exposed to elevated CO₂. *Science* 309: 1360–1362.
- Landhäusser SM, Chow PS, Dickman LT, Furze ME, Kuhlman I, Schmid S, Wiesenbauer J, Wild B, Gleixner G, Hartmann H *et al.* 2018. Standardized protocols and procedures can precisely and accurately quantify non-structural carbohydrates. *Tree Physiology* 38: 1764–1778.
- Lastdrager J, Hanson J, Smeekens S. 2014. Sugar signals and the control of plant growth and development. *Journal of Experimental Botany* 65: 799–807.
- Lauriks F, Salomón RL, Steppe K. 2021. Temporal variability in tree responses to elevated atmospheric CO₂. *Plant, Cell & Environment* 44: 1292–1310.
- Liesche J. 2017. Sucrose transporters and plasmodesmal regulation in passive phloem loading: mechanism and regulation of passive phloem loading. *Journal of Integrative Plant Biology* 59: 311–321.
- Lindeberg T. 2015. Image matching using generalized scale-space interest points. *Journal of Mathematical Imaging and Vision* 52: 3–36.
- Maier CA, Johnsen KH, Clinton BD, Ludovici KH. 2010. Relationships between stem CO₂ efflux, substrate supply, and growth in young loblolly pine trees. *New Phytologist* 185: 502–513.
- Martínez-Sancho E, Treydte K, Lehmann MM, Rigling A, Fonti P. 2022. Drought impacts on tree carbon sequestration and water use – evidence from intra-annual tree-ring characteristics. *New Phytologist*. doi: 10.1111/nph.18224.
- Martínez-Vilalta J, Sala A, Asensio D, Galiano L, Hoch G, Palacio S, Piper FI, Lloret F. 2016. Dynamics of non-structural carbohydrates in terrestrial plants: a global synthesis. *Ecological Monographs* 86: 495–516.
- Maxwell K, Johnson GN. 2000. Chlorophyll fluorescence – a practical guide. *Journal of Experimental Botany* 51: 659–668.
- McMurtrie RE, Dewar RC. 2013. New insights into carbon allocation by trees from the hypothesis that annual wood production is maximized. *New Phytologist* 199: 981–990.
- Muhr J, Messier C, Delagrangé S, Trumbore S, Xu X, Hartmann H. 2016. How fresh is maple syrup? Sugar maple trees mobilize carbon stored several years previously during early springtime sap-ascend. *New Phytologist* 209: 1410–1416.
- Murakami PF, Schaberg PG, Shane JB. 2008. Stem girdling manipulates leaf sugar concentrations and anthocyanin expression in sugar maple trees during autumn. *Tree Physiology* 28: 1467–1473.
- Niklas KJ. 1992. *Plant biomechanics: an engineering approach to plant form and function*. Chicago, IL, USA: University of Chicago Press.
- Norby RJ. 2021. Comment on “Increased growing-season productivity drives earlier autumn leaf senescence in temperate trees”. *Science* 371: eabg1438.
- O’Keefe J. 2019. *Phenology of woody species at Harvard Forest since 1990*. Harvard Forest Data Archive. [WWW document] URL <https://harvardforest.fas.harvard.edu/exist/apps/datasets/showData.html?id=hf003> [accessed 1 August 2022].
- Oribe Y, Funada R. 2017. Locally heated dormant cambium can re-initiate cell production independently of new shoot growth in deciduous conifers (*Larix kaempferi*). *Dendrochronologia* 46: 14–23.
- Oribe Y, Funada R, Shibagaki M, Kubo T. 2001. Cambial reactivation in locally heated stems of the evergreen conifer *Abies sachalinensis* (Schmidt) Masters. *Planta* 212: 684–691.
- Parent B, Turc O, Gibon Y, Stitt M, Tardieu F. 2010. Modelling temperature-compensated physiological rates, based on the co-ordination of responses to temperature of developmental processes. *Journal of Experimental Botany* 61: 2057–2069.
- Perez-Priego O, Guan J, Rossini M, Fava F, Wutzler T, Moreno G, Carvalhais N, Carrara A, Kolle O, Julitta T *et al.* 2015. Sun-induced chlorophyll fluorescence and photochemical reflectance index improve remote-sensing gross primary production estimates under varying nutrient availability in a typical Mediterranean savanna ecosystem. *Biogeosciences* 12: 6351–6367.

- Peters RL, Steppe K, Cuny HE, De Pauw DJW, Frank DC, Schaub M, Rathgeber CBK, Cabon A, Fonti P. 2020. Turgor – a limiting factor for radial growth in mature conifers along an elevational gradient. *New Phytologist* 229: 213–229.
- Peuke AD, Windt C, Van As H. 2006. Effects of cold-girdling on flows in the transport phloem in *Ricinus communis*: is mass flow inhibited? *Plant, Cell & Environment* 29: 15–25.
- Pugh TAM, Lindeskog M, Smith B, Poulter B, Arneith A, Haverd V, Calle L. 2019. Role of forest regrowth in global carbon sink dynamics. *Proceedings of the National Academy of Sciences, USA* 116: 4382–4387.
- Pugh TAM, Rademacher T, Shafer SL, Steinkamp J, Barichivich J, Beckage B, Haverd V, Harper A, Heinke J, Nishina K *et al.* 2020. Understanding the uncertainty in global forest carbon turnover. *Biogeosciences Discussions* 17: 3961–3989.
- Pya N. 2020. *SCAM: shape constrained additive models*. [WWW document] URL <https://cran.r-project.org/web/packages/scam/scam.pdf> [accessed 1 August 2022].
- R Core Team. 2019. *R: a language and environment for statistical computing*. Vienna, Austria: R Foundation for Statistical Computing.
- Rademacher T, Basler D, Eckes-Shephard AH, Fonti P, Friend AD, Le Moine J, Richardson AD. 2019. Using direct phloem transport manipulation to advance understanding of carbon dynamics in forest trees. *Frontiers in Forests and Global Change* 2: 11.
- Rademacher T, Fonti P, LeMoine JM, Fonti MV, Basler D, Chen Y, Friend AD, Seyednasrollah B, Eckes-Shephard AH, Richardson AD. 2021a. Manipulating phloem transport affects wood formation but not local nonstructural carbon reserves in an evergreen conifer. *Plant, Cell & Environment* 44: 2506–2521.
- Rademacher T, van Scoy M, Richardson AD. 2021b. *Impacts of phloem chilling on mature red maples at Harvard Forest 2019 (HF421)*. Harvard Forest Data Archive. [WWW document] URL <https://harvardforest1.fas.harvard.edu/exist/apps/datasets/showData.html?id=HF421> [accessed 1 August 2022].
- Rademacher T, Seyednasrollah B, Basler D, Cheng J, Mandra T, Miller E, Lin Z, Orwig DA, Pederson N, Pfister H *et al.* 2021c. The Wood Image Analysis and Dataset (WIAD): open-access visual analysis tools to advance the ecological data revolution. *Methods in Ecology and Evolution* 12: 2379–2387.
- Rathgeber CBK, Cuny HE, Fonti P. 2016. Biological basis of tree-ring formation: a crash course. *Frontiers in Plant Science* 7: 734.
- Regier N, Streb S, Zeeman SC, Frey B. 2010. Seasonal changes in starch and sugar content of poplar (*Populus deltoides* x *nigra* cv. Dorskamp) and the impact of stem girdling on carbohydrate allocation to roots. *Tree Physiology* 30: 979–987.
- Riou-Khamlichi C, Menges M, Healy JMS, Murray JAH. 2000. Sugar control of the plant cell cycle: differential regulation of *Arabidopsis* D-type cyclin gene expression. *Molecular and Cellular Biology* 20: 4513–4521.
- Rohde A, Bastien C, Boerjan W. 2011. Temperature signals contribute to the timing of photoperiodic growth cessation and bud set in poplar. *Tree Physiology* 31: 472–482.
- Rossi S, Deslauriers A, Griçar J, Seo J-W, Rathgeber CB, Anfodillo T, Morin H, Levanic T, Oven P, Jalkanen R. 2008. Critical temperatures for xylogenesis in conifers of cold climates. *Global Ecology and Biogeography* 17: 696–707.
- Salmon Y, Lintunen A, Dayet A, Chan T, Dewar R, Vesala T, Hölttä T. 2020. Leaf carbon and water status control stomatal and nonstomatal limitations of photosynthesis in trees. *New Phytologist* 226: 690–703.
- Servio P, Englezos P. 2001. Effect of temperature and pressure on the solubility of carbon dioxide in water in the presence of gas hydrate. *Fluid Phase Equilibria* 190: 127–134.
- Seyednasrollah B, Rademacher T, Basler D. 2021. bnasr/wiad: wood image analysis and dataset (WIAD) – source code. *Zenodo*. doi: [10.5281/zenodo.5272692](https://doi.org/10.5281/zenodo.5272692).
- Spicer R. 2014. Symplasmic networks in secondary vascular tissues: parenchyma distribution and activity supporting long-distance transport. *Journal of Experimental Botany* 65: 1829–1848.
- Teskey RO, Saveyn A, Steppe K, McGuire MA. 2008. Origin, fate and significance of CO₂ in tree stems. *New Phytologist* 177: 17–32.
- Thorpe MR, Furch ACU, Minchin PEH, Föllner J, Van Bel AJE, Hafke JB. 2010. Rapid cooling triggers forisome dispersion just before phloem transport stops. *Plant, Cell & Environment* 33: 259–271.
- Uggla C, Magel E, Moritz T, Sundberg B. 2001. Function and dynamics of auxin and carbohydrates during earlywood/latewood transition in scots pine. *Plant Physiology* 125: 2029–2039.
- Vaughn MW, Harrington GN, Bush DR. 2002. Sucrose-mediated transcriptional regulation of sucrose symporter activity in the phloem. *Proceedings of the National Academy of Sciences, USA* 99: 10876–10880.
- Vitasse Y, Lenz A, Körner C. 2014. The interaction between freezing tolerance and phenology in temperate deciduous trees. *Frontiers in Plant Science* 5: 541.
- Walker AP, Kauwe MGD, Bastos A, Belmecheri S, Georgiou K, Keeling RF, McMahon SM, Medlyn BE, Moore DJP, Norby RJ *et al.* 2021. Integrating the evidence for a terrestrial carbon sink caused by increasing atmospheric CO₂. *New Phytologist* 229: 2413–2445.
- Wiley E, Casper BB, Helliker BR. 2017. Recovery following defoliation involves shifts in allocation that favour storage and reproduction over radial growth in black oak. *Journal of Ecology* 105: 412–424.
- Wilson BF. 1968. Effect of girdling on cambial activity in white pine. *Canadian Journal of Botany* 46: 141–146.

Supporting Information

Additional Supporting Information may be found online in the Supporting Information section at the end of the article.

Notes S1 Notes on the experimental site including maps, sketches, and photographs of the site.

Notes S2 Notes on methods of anatomical analysis with high-resolution images of microcore sections.

Notes S3 Notes on tree water status including leaf and branch water potential, as well as sap flow measurements.

Notes S4 Notes on photosynthesis and fluorescence measurements including instantaneous photosynthetic rates at the top and bottom of the canopy, A/C_i curves, light response curves, and fluorescence measurements.

Please note: Wiley Blackwell are not responsible for the content or functionality of any Supporting Information supplied by the authors. Any queries (other than missing material) should be directed to the *New Phytologist* Central Office.